Earthquake triggering by static and dynamic stress changes

M. E. Belardinelli
Dipartimento di Fisica, University of Bologna, Italy

A. Bizzarri
Istituto Nazionale di Geofisica e Vulcanologia, Rome, Italy
Dipartimento di Fisica, University of Bologna, Italy

M. Cocco
Istituto Nazionale di Geofisica e Vulcanologia, Rome, Italy

Received 23 January 2002; revised 13 August 2002; accepted 9 October 2002; published 7 March 2003.

[1] In this study we aim to understand the effect of static and dynamic stress changes in promoting earthquake failures on secondary faults. Toward this goal we solve the equation of motion of a spring-slider dynamic system including inertia and using rate- and state-dependent constitutive laws. We separately investigate the dynamic response of this fault analog system to a sudden stress change represented either as a stress step or as a stress pulse, which are used to model permanent (static) and transient (dynamic) stress perturbations. The induced earthquake failure does not occur immediately at the application of the coseismic stress change, but it is delayed in time: we define this time interval as the triggering delay. For a given stress perturbation, we analyze the dependence of triggering delays on different system conditions and constitutive parameters. Our results clearly show that the effects of static and dynamic stress changes are quite different. While a static stress change is able to advance as well as to delay an induced instability depending on its sign, a dynamic stress pulse is only able to promote a nearly instantaneous failure, provided its amplitude is positive and large enough with respect to the direct effect of friction. In other words, dynamic stress changes can only cause nearly instantaneous failures, without any relevant triggering delay. These results should be considered in interpreting the seismicity rate changes caused by large earthquakes at least as long as seismic events are interpreted as sliding instabilities obeying rate- and state-dependent friction laws. *INDEX TERMS:* 7209 Seismology: Earthquake dynamics and mechanics; 7260 Seismology: Theory and modeling; 7299 Seismology: General or miscellaneous; *KEYWORDS:* stress trigger, fault interaction, rate- and state-dependent friction, spring-slider

Citation: Belardinelli, M. E., A. Bizzarri, and M. Cocco, Earthquake triggering by static and dynamic stress changes, *J. Geophys. Res.*, *108*(B3), 2135, doi:10.1029/2002JB001779, 2003.

1. Introduction

[2] Observations and theoretical models support the idea that earthquakes perturb the state of stress of neighboring faults [*Harris*, 1998; *Stein*, 1999; *King and Cocco*, 2000]. These perturbations are represented by coseismic stress changes which modify the mechanical conditions of active faults yielding induced earthquake failures that can be advanced as well as delayed in time with respect to the unaltered (unknown) occurrence of seismic events. In this context, ''induced'' events are those whose failure times have been advanced (or delayed) with respect to the unperturbed stressing. Near the causative faults, the induced coseismic stress field consists both of transient (dynamic) and permanent (static) stress changes. While at remote distances transient stresses are dominant [*Rybicki et al.*, 1985; *Cotton and Coutant*, 1997; *Gomberg et al.*, 1997, 1998], in the near-field these two factors cannot be separated and they act together in triggering impending earthquakes [see *Harris*, 1998; *Belardinelli et al.*, 1999; *Gomberg et al.*, 2000]. In this study we investigate the fault dynamic response to transient and permanent stress changes in order to understand if these two stress perturbations have the same capability to modify the mechanical conditions of active faults and to shed light on the physical processes underlying earthquake triggering. *Gomberg* [2001] discussed a similar problem with simple heuristic models presenting conflicting evidence on earthquake failure models. Here, we aim to contribute to this discussion by presenting numerical calculations and simulations to answer to this stimulating open question.

[3] The 1992 Landers earthquake provided the first striking examples of short- and long-range interactions,

0148-0227/03/2002JB001779$09.00

which were interpreted to support both static and dynamic triggering. Dynamic stress changes associated with the passage of seismic waves have been proposed to explain remotely triggered seismicity both after the 1992 Landers earthquake [*Hill et al.*, 1993] and the 1999 Izmit event [*Brodsky et al.*, 2000]. Recently, *Kilb et al.* [2000] suggested that dynamic stress changes, rather than static perturbations, better explain the distribution of the aftershocks that occurred within about 10 months following the 1992 Landers earthquake. This result implies that dynamically triggered events can occur at any time after the seismic waves have passed and even with considerable delay [see also *Gomberg et al.*, 1997, 1998]. In order to detect dynamic triggering, it is necessary to observe that the rate of earthquakes after the passage of seismic waves is larger than the rate of events before the transient perturbation. Dynamic triggering due to long range interactions can be verified and tested in a statistical sense only in a specified time window starting immediately after the arrival of the stress perturbation and lasting for days to months [*Hill et al.*, 1993]. This time window is therefore much longer than the persistence of the stress perturbation. In the near field, however, it can be extremely difficult to test statistically if the dynamic stress perturbations can alter the aftershock distribution and the seismicity rate, because their effects on the rate of earthquake production may be indistinguishable from those caused by static stress changes.

[4] A particular goal of the present study is therefore to understand if dynamic stress changes can promote subsequent earthquakes at any time after the induced perturbation. In performing this investigation, we have to account for the fault constitutive properties and their variability [*Gomberg et al.*, 1998; *Belardinelli et al.*, 1999; *King and Cocco*, 2000]. We represent the fault frictional properties by using a rate- and state-dependent constitutive formulation [*Dieterich*, 1979, 1986; *Ruina*, 1980, 1983]. According to this description, *Scholz* [1998] proposed the earthquake insensitivity to dynamic transient stresses: The direct effect of friction and the finite size and duration of nucleation prohibit earthquakes from being triggered by high-frequency stress changes. These considerations emphasize that there is no general agreement on the role played by dynamic stress changes. We aim to clarify this controversy by investigating the dynamic response of a spring-slider system including inertia to transient and permanent changes of the external loads.

2. Simulation Strategy

[5] In this study we numerically solve the equation of motion of a spring-slider dynamic system (see Figure 1) including inertia

$$m\ddot{\delta} = \tau + \Delta\tau(t) - \tau_f$$

where δ is the slip, m is the mass per unit surface, τ_f is the frictional resistance and τ is the elastic traction on the slider. If δ_0 is the displacement of the loading point moving at constant velocity $V_0 = \dot{\delta}_0$ and k is the elastic spring constant, then $\tau = k(\delta_0 - \delta)$. The term $\Delta\tau(t)$ represents the time-dependent stress perturbation of the slider traction, such as that caused by a nearby earthquake. The stress

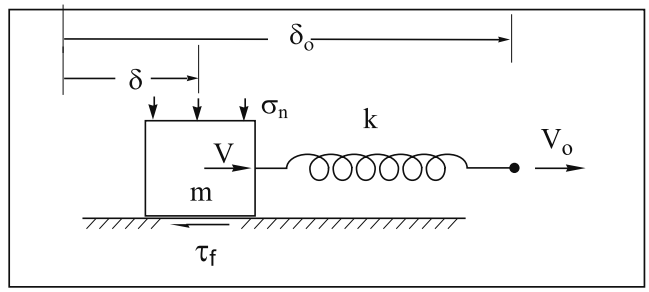

Figure 1. Schematic representation of a spring-slider system.

perturbation $\Delta\tau(t)$ is assumed to be zero for times less than or equal to the external load application time (named the onset time in the remainder of the paper). The use of a spring-slider model to study earthquake triggering assumes that the nucleation patch, which has its own finite size, is a single degree of freedom dynamic system. Although a spring-slider analog model is a simplistic representation of an active fault, it allows modeling of repeated seismic events accounting for fault constitutive properties (fault restrengthening) and stress perturbations during the seismic cycle. For these reasons, it has been widely used in the literature [*Rice and Gu*, 1983; *Roy and Marone*, 1996; *Boatwright and Cocco*, 1996; *Gomberg et al.*, 1997, 1998, 2000, among many others].

[6] In this study we use the simulation strategy proposed by *Boatwright and Cocco* [1996], which uses the quasi-static approximation at low values of the sliding velocity, $V = \dot{\delta}$. The equation of motion becomes

$$\tau + \Delta\tau(t) = \tau_f, \quad V \le V_c,$$

where V_c is a suitable value of the slider velocity [*Rice and Tse*, 1986]. We have chosen $V_c = 100$ μm/s to separate two constitutive regimes: the first one ($V \le V_c$) in which we solve the dynamic equation system with the quasi-static approximation and the other ($V > V_c$) where we include inertia and the motion is fully dynamic. We use rate- and state-dependent constitutive laws with both a slowness (Dieterich-Ruina) evolution equation, which implies true ageing

$$\tau_f = \tau_* + A\ln\left(V/V_*\right) + B\ln\left(V_*\xi/L\right)$$
$$\dot{\xi} = 1 - V\xi/L \qquad (1)$$

as well as a slip (Ruina) evolution equation [see *Beeler et al.*, 1994]

$$\tau_f = \tau_* + A\ln\left(V/V_*\right) + \Theta$$
$$\dot{\Theta} = -\frac{V}{L}\left[\Theta + B\ln\left(\frac{V}{V_*}\right)\right] \qquad (2)$$

[7] In these equations, the constitutive parameters are $A = a\sigma_n$, $B = b\sigma_n$ and L, σ_n being the normal stress. The first equation in equations (1) and (2) relates fault friction to the sliding velocity and the state variable and is usually named the governing equation. The second relation represents the

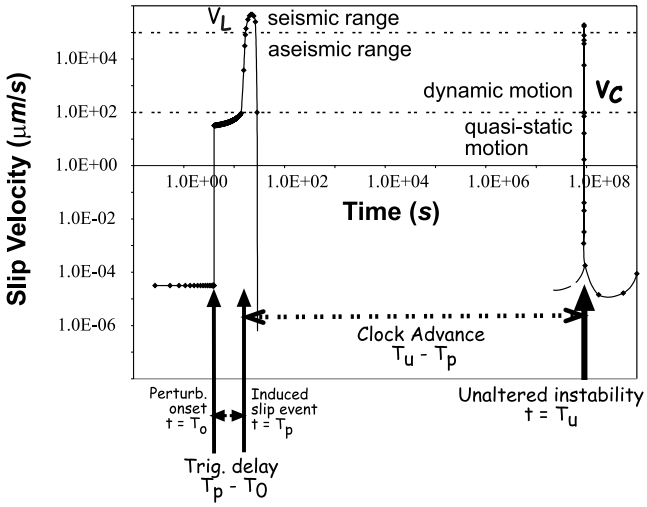

Figure 2. Sliding velocity as a function of time caused by a stress step perturbation $\Delta\tau_S$ of 12.4 bars applied at the onset time $T_0 = 1.25$ s after the beginning of the simulation. We used the slip law and the set of parameters listed in Table 1 (set 1) except for $T_{a,f} = 25$ s and $\dot{\tau}_0 = 1.5 \times 10^{-8}$ bars/s. The initial friction is taken as the steady-state value for the assumed initial velocity. T_p is the failure time under perturbed conditions, while T_u is that in unaltered conditions. A dynamic instability is identified when the system exceeds the limiting velocity V_L, defined as an assumed threshold $V_L = 10$ cm/s. The triggering delay $t_p = T_p - T_0$ and the clock advance $t_u = T_u - T_p$ are graphically defined here. $V_c = 100$ μm/s is the value of the slider velocity chosen to separate the quasi-static from the dynamic response (see text for the details). After the abrupt velocity change caused by the static stress step, the slip velocity slowly increases before the dynamic instability.

temporal evolution of the state variable and it is named the evolution equation. The term $A = a\sigma_n$ accounts for the direct effect of friction, which is the sudden increase in friction caused by a sudden change in sliding velocity [see *Scholz*, 1990, and references therein]. For both constitutive formulations considered here, the constitutive parameters B and L control the evolution of the state variables ξ and Θ [see *Ruina*, 1980, 1983], which account for the properties of contact sliding surfaces. The evolution equations provide a time-dependence to fault friction and the state variables represent a memory of previous slip episodes. We numerically solve the equation of motion under unsteady conditions $\dot{\xi} \neq 0$ and $\dot{\Theta} \neq 0$, and therefore in our simulations, the state variable is always evolving from its initial value.

[8] Following *Weeks* [1993] we assume that, for both the constitutive laws considered in this study, friction becomes independent of velocity at high slip rates and we solve the equation of motion by using the following relation

$$A \ln\left(V/V_*\right) = A \ln\left(V_c/V_*\right) \quad \text{for } V > V_c$$

[see *Boatwright and Cocco*, 1996]. We also consider the case, for the slowness evolution law (1), in which no constraints exist at high slip rates. This allows us to check the effect of friction behavior at high sliding velocities that we will discuss in the following section.

[9] In most of the cases considered here, the spring-slider parameters are chosen to make unstable the equilibrium state of the quasi-static system, which requires a stiffness smaller than its critical value $k < (B - A)/L$ [see *Gu et al.*, 1984]. The system in this case spontaneously becomes unstable in a finite time, even when unperturbed ($\Delta\tau(t) \equiv 0$) with only the loading rate transmitted by the spring. During the instability, the slider velocity reaches very large values compared to the loading point velocity. In this model, the loading rate transmitted by the spring ($\dot{\tau}_0 = kV_0$) is representative of remote tectonic loading and the instability represents a seismic event. We identify a seismic slip event, or an instability, when the slip velocity becomes transiently larger than an assumed threshold $V_L = 10$ cm/s (Figure 2). An earthquake can thus be expected in our model also in unperturbed conditions. We refer to the instability occurring for $\Delta\tau(t) = 0$ as an unaltered or unperturbed dynamic event. We indicate the time of application of the induced perturbation (onset time) as T_0, while the occurrence time of the instability is $T_u > T_0$ for unperturbed load conditions, and $T_p > T_0$ for perturbed system. The triggering delay is here defined as $t_p = T_p - T_0$ and the unperturbed time delay is defined as $t_u = T_u - T_0$ (see Figure 2). In the long term the slider is characterized by velocity and friction values that vary periodically with time, provided that $k < (B - A)/L$. The period of this variation defines the slider cycle time T, which is associated with the earthquake recurrence time on the same fault. The cycle of the system is represented by the phase diagram [see *Gu et al.*, 1984; *Rice and Tse*, 1986, among several others] which, for a spring-slider model (with a single state variable), plots friction as a function of the logarithm of the slider velocity. We plot in Figure 3 an example of a phase diagram corresponding to the slider cycle and we indicate with a color scale the temporal evolution of the dynamic system. In this case it is possible to associate a particular set of the system conditions at the onset time to a particular stage along the seismic cycle.

[10] The occurrence times T_p and T_u can be compared assuming the same system conditions at a time t_0 less than or equal to the application time of the induced load (T_0). In fact, to study the evolution of a dynamic system it is necessary to know the state at an arbitrary instant of time t_0, called here the reference time. The system evolution for $t > t_0$ depends on the system conditions at the reference time (i.e., the reference state), which control the occurrence of instability under both unaltered and perturbed conditions when a known perturbation is applied at a time $T_0 \geq t_0$. Thus, both T_p and T_u depend on the reference state, unlike the cycle time. The system evolves to its cycle (Figure 3) after losing memory of the reference state, as we will see in the next sections. The cycle time cannot be obtained using spring-slider models which neglect inertia and for this reason previous analyses [*Gomberg et al.*, 1998, 2000], which used a quasi-static solution, identified the cycle time with the time T_u of the unaltered slip instability. We emphasize that only the unperturbed time delay T_u depends on the reference state. In the following we will identify the reference state with the state of the system at the onset time T_0, immediately before the application of the stress perturbation.

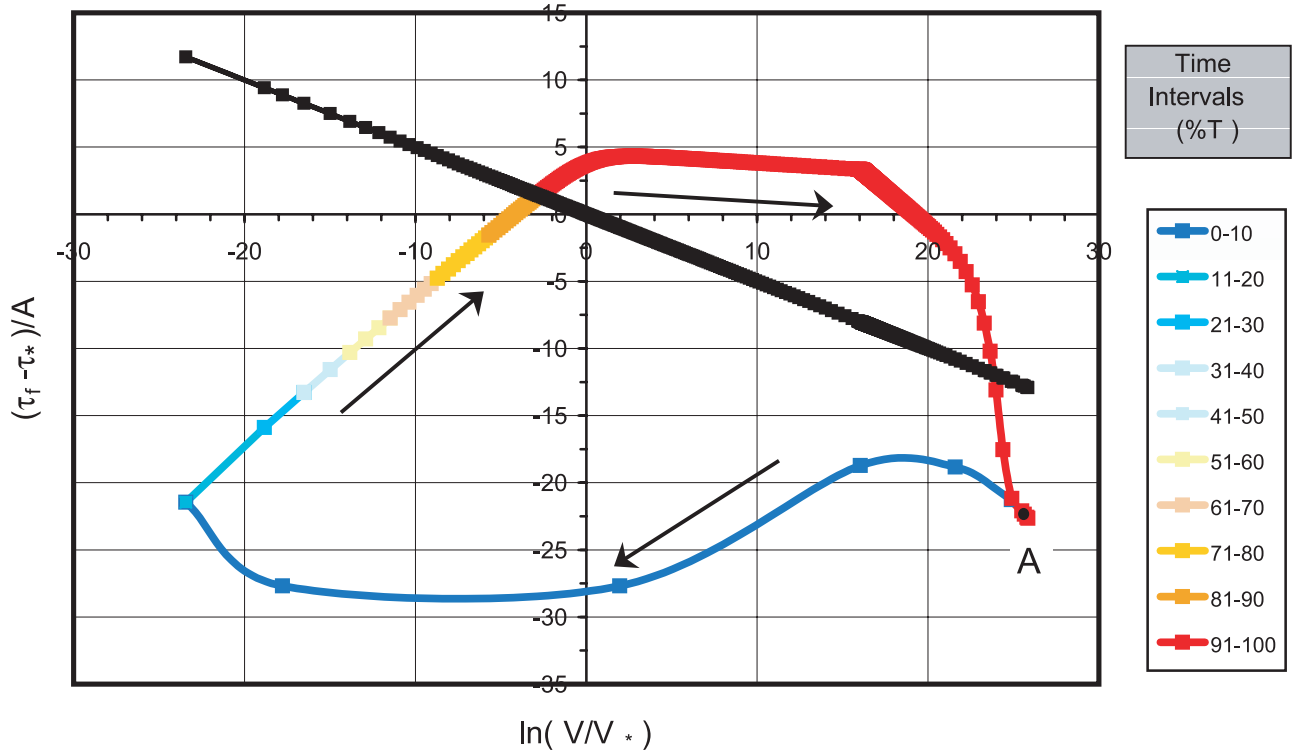

Figure 3. Plot of the closed trajectory (cycle) in the phase plane followed by the system in unperturbed conditions. We used the slowness law and the parameter values reported in set 1 of Table 1 and plotted the system trajectory after a few instabilities, when it has lost its memory of the initial conditions. Each state on the cycle is occupied at a given instant of time shown by the color scale. The system runs along the whole trajectory in a time interval equal to the cycle period T. Times are computed from the last time at which the system reached the maximum velocity (occupying the state marked by A in the phase diagram). They are expressed as a percentage of the cycle period from blue to red in the color scale. The direction of motion along the trajectory is indicated by the arrows.

[11] We will investigate under which circumstances the triggering delay is smaller than the unperturbed time delay, in this case we assert that the stress perturbation promoted the earthquake. Alternatively, following *Gomberg et al.* [1997, 1998], the amplitude of the clock advance, $T_u - T_p$, can be used to claim whether an earthquake is promoted by a stress perturbation. However, we believe that the estimate of the triggering delay is more practical than the estimate of the clock advance in earthquake triggering studies, since it provides T_p with respect to a known reference time T_0. The goal of the paper is to provide some modeling results that support the possibility of earthquake triggering on timescales much shorter than the recurrence time of earthquakes on a specific fault. To this aim, we investigate the resulting triggering delays for different applied loads, constitutive parameters and system conditions at the onset time.

3. Response to a Step Stress Change

[12] We first investigate the dynamic response of the spring-slider system to a stress change represented analytically by a step function with a prescribed height (see Figure 4), according to the following expression

$$\Delta\tau(t) = \Delta\tau_S\left[r - e^{-(t-T_0)/p}\right] \quad \text{with } t > T_0 \tag{3}$$

[13] A sudden stress step equal to $\Delta\tau_S$ can be modeled assuming $r = 1$ and $p = 10^{-3}$ s in equation (3), and it represents an induced static stress change. Figure 4 shows an example of dynamic response to a step stress change. We perturb the system a few seconds after the beginning of the simulation, starting the simulation at an initial state characterized by steady-state friction $\tau_f = \tau_{SS}(V_s)$ at the assumed initial velocity V_s, where the steady-state friction at a general sliding velocity V is defined as follows

$$\tau_{SS}(V) = \tau_* + (A - B)\ln\left(V/V_*\right) \tag{4}$$

[14] Therefore, the system state at the time of application of the stress perturbation (i.e., the onset time T_0) can be approximated with the initial conditions at the beginning of the simulation (in particular, $V(T_0) \cong V_s$). This is the case for all the simulations discussed in this paper unless differently specified. We will discuss in a different section the results of numerical simulations performed by applying the stress perturbation during the cycle of the slider. Figure 4 shows that a positive stress step $\Delta\tau_S$ suddenly increases the slider velocity, leaving the state variable value unchanged. The values of initial and constitutive parameters used for the simulation shown in Figure 4 are listed in Table 1 (parameter set 1). According to the quasi-static approximation, we can thus estimate the

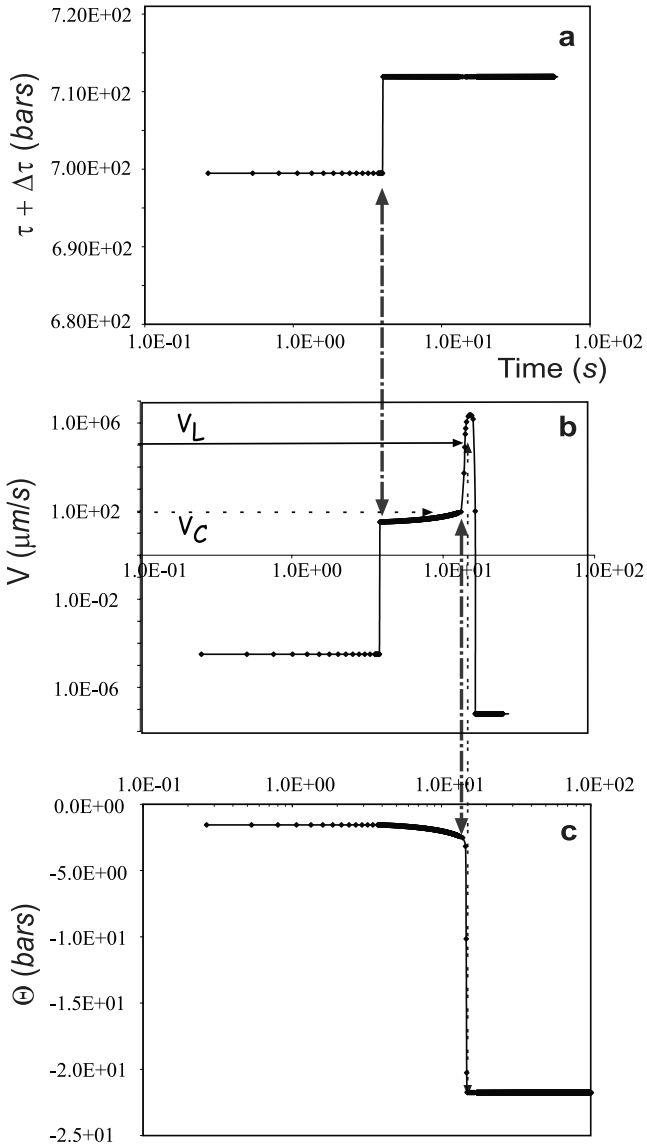

Figure 4. (a) Slider response to the stress step change. (b) The slip velocity shown as a function of time. (c) The state variable shown as a function of time. We adopt a slip evolution law; the initial and constitutive parameters are those listed in set 1 of Table 1. The initial friction is the steady-state value corresponding to the assumed initial velocity. The slider response to an abrupt stress change is a sudden step followed by a continuous increase in sliding velocity, which is driven by the state variable evolution. The dynamic instability occurs when the state variable abruptly drops to a new steady-state value and the sliding velocity suddenly increases to a dynamic failure.

slip velocity response due to the stress step as $V(T_0^+)$, where $T_0^+ - T_0 \sim p$ and

$$V(T_0^+) \cong V(T_0)e^{(\Delta\tau_S/A)} \tag{5}$$

[15] Our results show that in general, if $\Delta\tau > 0$, this perturbation of the sliding velocity is sufficient to advance the next instability, i.e., $t_p < t_u$. The sudden change in slip velocity increases with the applied stress-step amplitude $\Delta\tau_S$. This explains why the triggering delay decreases for increasing values of $\Delta\tau_S$, as will be shown in the following sections. On the contrary negative stress step changes suddenly decrease the slider velocity delaying the onset of the subsequent instability with respect to the unperturbed one, i.e., $t_p > t_u$.

Table 1. Parameters Used for the Calculations Shown in the Figures

	Set 1	Set 2	Set 3	Set 4
A, bars	0.9	5	5	0.9
B, bars	1.35	10	7.5	1.35
V_*, μm/s	10^{-5}	10^{-4}	10^{-5}	10^{-5}
L, μm	10^4	10^3	10^4	10^4
k, bars/μm	10^{-5}	1.25×10^{-4}	10^{-5}	10^{-5}
T_{af}, s[a]	5	5	5	5
$\dot{\tau}_0$, bars/s[b]	1.5×10^{-9}	1.25×10^{-8}	1.5×10^{-9}	3×10^{-8}
τ_*, bars	700	700	700	700
V_s, μm/s	3.17×10^{-5}	10^{-4}	3.17×10^{-5}	3×10^{-4}

[a] $T_{af.} = 2\pi\sqrt{m/k}$ is the period of the analogous freely slipping system [*Rice and Tse*, 1986].
[b] $\dot{\tau}_0 = k\dot{\delta}_0$ is the tectonic loading rate.

[16] A rate- and state-dependent formulation with a slip evolution equation (2) has been used for the simulations shown in Figure 4, assuming that friction becomes independent of slider velocity at high slip rates ($V > V_c$). In Figure 5, we compare the response of the spring-slider system to the same perturbation used in Figure 4 (a static step stress change $\Delta\tau_S = 12.4$ bars) for both the constitutive laws described before (equations (1) and (2)); for the slowness law (1), we also considered the case in which friction becomes independent of velocity at high slip rates. This figure clearly shows that the choice of the constitutive law affects the resulting time of occurrence of the promoted instability. Moreover, the friction behavior at high slip rates also modifies the slider response: The transition from the quasi-static to the fully dynamic regime depends on the friction behavior at high slip rates, as shown in Figure 5. This implies that the value of the triggering delay depends

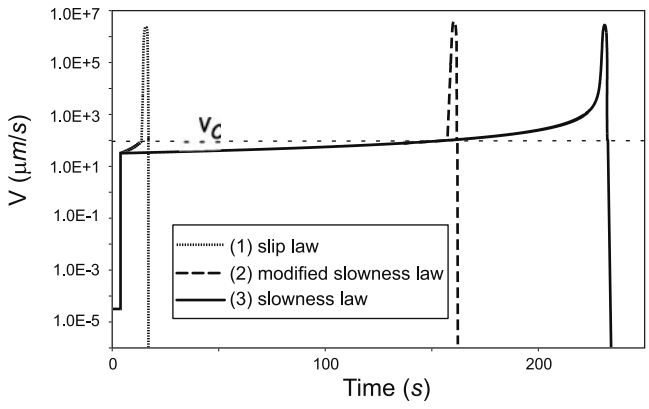

Figure 5. Dynamic response to a stress step perturbation $\Delta\tau_s$ of 12.4 bars of a spring slider obeying different constitutive laws: (1) a slip law (equation (2)) and a slowness law (equation (1)) (2) modified and (3) not modified at high slip rates for $V \geq V_C$ (see text for more details). Initial and constitutive parameters are as in Figure 3.

on the adopted law and on the friction behavior at high slip velocity for the same set of constitutive parameters and system conditions at the onset time. This is in agreement with previous results presented by *Roy and Marone* [1996]. For the slowness law, the friction behavior at high slip rates entails differences of the order of tens of seconds in the triggering delays, regardless of the system parameters, system conditions at the onset time and stress perturbation parameters. Thus, it produces a minor effect with respect to the choice of the constitutive law, which causes larger differences in the computed triggering delays.

[17] According to equation (5), the change of slip velocity depends on the stress amplitude, the constitutive parameters, and the system conditions at the onset time. We can thus expect that the triggering delays also depend on the same parameters and on the system conditions at the onset time. We will discuss separately these effects in the following sections.

4. Response to a Pulse Stress Change

[18] In this section we discuss the response of the spring-slider system to a transient stress change represented by a Gaussian pulse, whose analytic expression is given by

$$\Delta\tau(t) = \Delta\tau_G \cdot e^{-(t-T_0-3\sigma)^2)/(2\sigma^2)} \quad \text{with } t > T_0 \qquad (6)$$

where $\Delta\tau_G$ is the stress peak. The pulse is centered on $T_0 + 3\sigma$ and the pulse width is approximately given by 6σ. Figure 6 shows an example of the slider response to a stress perturbation represented by a gaussian pulse whose peak is $\Delta\tau_G$ = 12.4 bars. The initial conditions of the system are characterized by the steady-state value of friction at the assumed initial velocity V_s and we perturb the system few seconds after the beginning of the simulation, as in Figure 4. We use the slip evolution equation with the same constitutive parameters (see Table 1) of Figure 4. This transient load is unable to promote a dynamic instability: It is evident that the applied stress change perturbs the system, which undergoes a transient slip episode of relatively high slip velocity and follows quite closely the applied stress time history. We will refer to this feature as "the instantaneous response", which might be interpreted as triggered aseismic slip or creep in the case of Figure 4. We also note that this dynamic (pulse-like) stress perturbation leaves the slider velocity for $t > T_0 + 6\sigma$ almost unaltered. Actually, the slip velocity time history shown in Figure 6 closely follows the time evolution of the external load (see Appendix A). We can conclude that, unlike static stress changes of similar amplitudes (see Figure 4), the dynamic pulse is unable to significantly and permanently modify the loading stress and the velocity of the system. The state variable is slightly decreased at the end of the stress perturbation, allowing the aseismic instantaneous response during the fully dynamic motion (shown in Figure 6). This variation, however, is very small if compared to that caused by the step stress change instability shown in Figure 4. The simulations shown in Figures 4 and 6 lead us to conclude that the response of the slider to static and dynamic induced stress changes of the same amplitude, for the same set of constitutive parameters and system conditions at the onset time, is quite different.

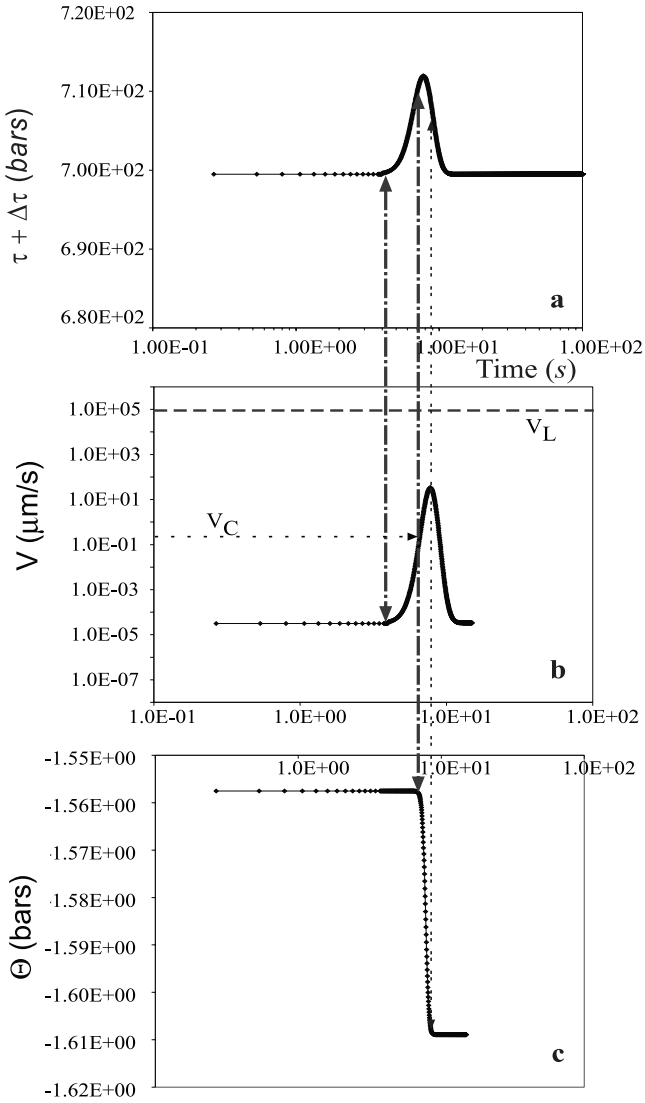

Figure 6. (a) Response to the stress pulse perturbation. (b) The slip velocity shown as a function of time. (c) The state variable shown as a function of time. The constitutive law and the initial and constitutive parameters are as in Figure 4. The amplitude of stress pulse $\Delta\tau_G$ is equal to that of the stress step $\Delta\tau_S$ used in Figure 4.

[19] We have performed many simulations with different constitutive parameters and system conditions at the onset time. In the present study we will not discuss in detail the effect of pulse duration 6σ; our results agree with those of *Gomberg et al.* [1997, 1998], which show that the frequency content of the transient loads also contribute to the triggering delay. In particular, for pulse durations smaller than 500 s, the triggering delay increases almost linearly with the pulse duration (except when the pulse duration becomes very large), if the dynamic instability occurs within the pulse duration time interval. Our results show that transient stress changes can promote such an effect or, in general, a nearly "instantaneous" triggering effect ($t_p \approx 0 \ll t_u$) only for very large values of the applied stress amplitude. In other words, the instantaneous response of the slider reaches slip-velocity values of the order of V_L only if the stress

perturbation is larger than the constitutive parameter A ($\Delta\tau_G \gg A = a\sigma_n$). In the opposite case ($\Delta\tau_G \leq A = a\sigma_n$), we found that pulse-like stress changes do not promote dynamic instabilities, but they might trigger aseismic slip episodes; in this case the instability following the application of the perturbation occurs very close in time to the unperturbed failure episode. We define this case as the "null" triggering effect ($t_p \cong t_u$).

[20] These results are summarized in Figure 7, where we show the triggering delay as a function of the pulse amplitude. This figure points out that the triggering delay (t_p) remains close to the unperturbed time delay (t_u) for a large range of values of $\Delta\tau_G$ (the null triggering effect), but it becomes very small ($t_p \cong 0$) for large values of the induced stress peak (the instantaneous triggering). This transition is very sharp and may be discontinuous for this particular system; it suggests the existence of a stress threshold [see *Harris*, 1998] separating the field of null triggering from the instantaneous triggering. In other words, we were unable by applying a stress pulse change to have triggering delays very different from the nearly instantaneous ($t_p \approx 0 \ll t_u$) or the unperturbed ($t_p \cong t_u$) values. For the simulations shown in Figure 7, performed by using a slip evolution equation modified at high slip rates, the threshold in the step stress amplitude is nearly equal to 13.5 bars. This value coincides with the maximum value of the increment of the direct effect of friction starting from the onset time, that is $A \ln(V_c/V_i)$ = 13.5 bars (the onset time velocity is estimated as $V_i \cong V_s$ and V_s and A are evaluated from the parameter values listed in Table 1). We obtained similar behavior with the slowness law either with or without modification at high slip rates. The minimum amplitude of dynamic stress promoting instantaneous failures depends on the assumed value of the limiting velocity V_L, the stress pulse parameters (e.g., σ), the system conditions at the onset time and the constitutive parameters. In general, perturbing the system from slip velocities smaller than 1 cm/yr and considering an onset time state close to the steady state, we found that the values of $\Delta\tau_G$ causing an instantaneous seismic event are very large compared to the direct effect of friction A, as evident in Figure 7. Our results show that the threshold value is larger than $A \ln(V_c/V_i)$ when the direct effect of friction is not frozen at high velocity.

[21] We can conclude that dynamic stress changes are likely to cause induced instabilities only with very short triggering delays ($t_p \approx 0 \ll t_u$, here called the instantaneous triggering effect), or do not produce relevant modifications to the system time response ($t_p \approx t_u$, here called the null triggering effect). We will further discuss and interpret this conclusion in the following sections.

5. The Effect of the System Conditions at the Onset Time

[22] We identify the mechanical conditions of the slider immediately before the application of the induced stress change (called here the onset time T_0) as a reference state for modeling the evolution of the dynamic system, as previously discussed. It is sufficient to know the mechanical state of the system at the time of application of the induced load to predict its response. The mechanical conditions of a fault are completely represented by the state of the dynamic system that, in the framework of rate- and state-dependent constitutive laws, can be represented by the values of sliding velocity, of the state variable and of the traction applied on the slider. In this study the dependence on the system conditions at the onset time is investigated for different constitutive parameters and stress time histories (transient and permanent induced loads).

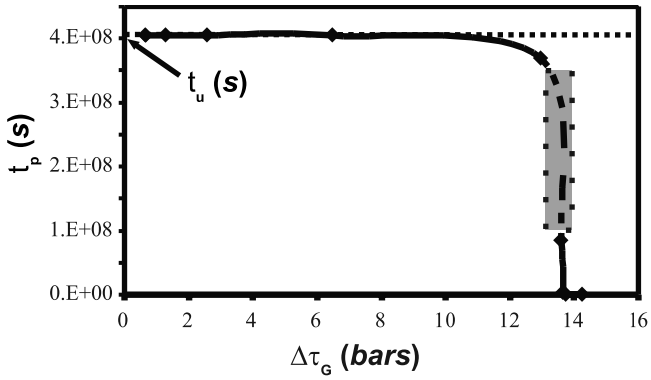

Figure 7. Triggering delay as a function of the stress pulse peak $\Delta\tau_G$. The pulse duration is 6σ = 7.5 s. The constitutive law and the initial and constitutive parameters are same as in Figure 6. The triggering delay is indistinguishable from the unperturbed time delay for a large interval of $\Delta\tau_G$ values (null effect), but for large values of the stress pulse amplitude ($\Delta\tau_G$ > 13.5 bars), it is of the order of seconds and comparable to the duration of the transient stress perturbation (instantaneous effect). The transition between null and instantaneous effects is very steep and occurs for a specific range of peak stress amplitudes that approximate the maximum friction increase due to the direct effect. The gray box shows the range of triggering delays, comprised between the unperturbed and the instantaneous time response (both values depending on the constitutive law, the system parameters and the system conditions at the onset time), that are not likely to occur after a pulse stress change.

[23] In most of the solutions presented in this study, the onset time is taken to be a few seconds after the beginning of the simulation. Therefore, the state assumed at the beginning of the simulation, called here the initial state of the system, well approximates the state at the onset time (OTS). We always started our simulations in quasi-static conditions (with initial velocity values $V_s < V_c$). The state of the slider in the quasi-static approximation is fully represented by the values of the slip velocity and friction. Thus, the initial quasi-static state of the system is defined by the velocity (V_s) and the friction (τ_s) values assumed at the beginning of the simulation, which in our calculations well approximate the values at the onset time $V(T_0) \equiv V_i$, $\tau_f(T_0) \equiv \tau_i$ [i.e., $V_i \cong V_s$ and $\tau_i \cong \tau_s$]. Accordingly, in order to vary the OTS in all of the cases considered in the previous and in the present sections, we have varied the velocity and/or friction values assumed at the beginning of the simulation. Our simulations clearly show that, for most of the adopted OTS and constitutive parameters, the slider evolution after a transient load does not differ substantially from the unperturbed evolution. This means that dynamic transient stress changes are generally unable to permanently and signifi-

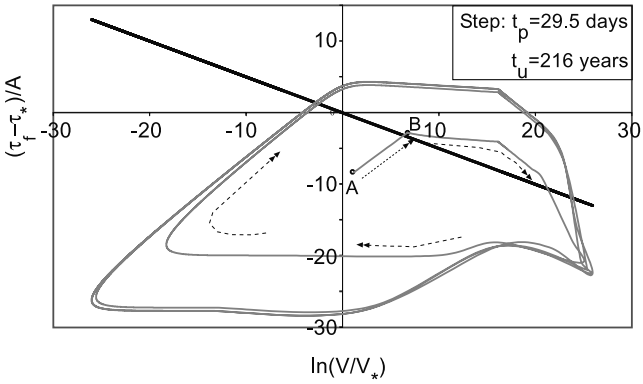

Figure 8. Phase diagram showing the dynamic response of a spring slider to a stress step $\Delta\tau_S$ of 5 bars. The system trajectory (gray line) begins in A (onset time state) and is moved to the state B (slightly above the steady-state line) by the applied external stress perturbation. Then, the system remains above the steady-state line (solid line). The dashed arrows indicate the direction of motion along the system trajectory. The onset time state can be approximated by the initial state, which is represented by a friction equal to 99% of the steady-state friction value at the assumed initial velocity (see set 1 in Table 1). The slowness ageing law not modified at high velocity was used. The unperturbed time delay is 216 years (indicated).

cantly modify the mechanical state of the slider. In these circumstances the triggering delay does not differ significantly from the unperturbed time delay, as we will show later in this section.

[24] Each couple of friction and velocity values (V, τ_f) identifies a point in the phase diagram shown in Figure 3 [see *Gu et al.*, 1984; *Rice and Tse*, 1986 for further details], which can lie above or below the steady-state stress level (the solid straight line in Figure 3). We show in Figure 8 an example of a phase diagram showing the slider response to a stress step of $\Delta\tau_S$ = 5 bars and for an OTS characterized by a friction value τ_i corresponding to 99% of the steady-state friction value at the assumed onset time velocity V_i (solid circle A). We perform this analysis considering the slowness law without any constraint at high slip rates. The black straight line represents the steady-state line, thus the OTS considered here lies below the steady-state curve. Figure 9 shows a similar test for the response to a gaussian pulse of $\Delta\tau_S$ = 5 bars and for an OTS (solid circle A) characterized by a friction value τ_i corresponding to 99.5% of the steady-state friction value at the assumed onset time velocity V_i. The two different initial states assumed for Figures 8 and 9 imply different values of the unperturbed time delays (216 and 126.2 years, respectively). In Figure 8, we can note the state of the system is strongly perturbed by the stress change (the system is moved from the state A to state B above the steady-state line at the end of stress perturbation). Accordingly the triggering delay is much different from the unperturbed time delay. On the contrary, in Figure 9 the dynamic state of the system is not significantly or permanently perturbed by the applied stress change. The system trajectory in Figure 9 starts from state A and reaches state B when the stress perturbation reaches its maximum value, but at the end of the pulse stress change the system returns to a state A′ very close to state A. This explains why in Figure 8 we find that t_p is significantly different from t_u whereas in Figure 9 we have $t_p \cong t_u$. With a similar reasoning we can interpret the results shown in Figures 4 and 6.

[25] In order to perform a systematic investigation of the effects of the assumed OTS on the triggering delay caused by permanent and transient induced loads, we have chosen numerous states of the dynamic system in the phase diagram plotted in Figures 8 and 9. Assuming that $k < (B - A)/L$, the equilibrium state of the system ($V = V_0$, $\tau_f = \tau_{SS}(V_0)$) is unstable and cannot be considered a long-term natural state of the system. We have performed many different tests with a static stress change and a stress pulse of the same amplitude equal to 5 bars, varying the distance of the OTS, (V_i, τ_i) from the steady-state curve, for the same velocity V_i. We used the three distinct sets of constitutive parameters listed in Table 1 (sets 1, 2, and 3). Set 2 corresponds to that used by *Gomberg et al.* [1998] if a value of σ_n = 100 MPa is assumed. Figure 10 shows the resulting time delay as a function of the frictional resistance τ_i. The latter is represented as the percentage of the steady-state stress $\tau_{SS}(V_i)$ at the velocity value V_i assumed at the onset time (values smaller or larger than 100% indicate stresses below or above the steady-state friction, respectively). Both the unperturbed time delays and the triggering delays associated with the two stress perturbation are reported in Figure 10, even if, as expected, the triggering delay associated with the stress pulse does not differ from the unperturbed time delay. This means that in all cases

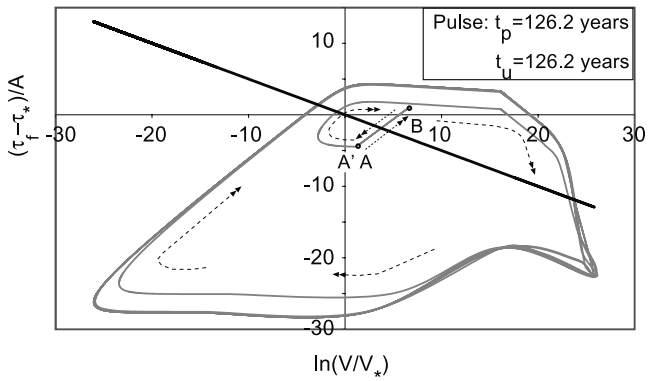

Figure 9. Phase diagram showing the dynamic response of a spring slider to a stress pulse $\Delta\tau_G$ of 5 bars and duration 6σ = 11.25 s. The system trajectory starts in A (onset time state) and reaches the maximum velocity in B when the applied stress is at its peak. Then the system goes back to a state A′ very close to the onset time state A and the trajectory transiently remains below the steady-state line. The onset time state can be approximated by the initial state, which is represented by a friction equal to the 99.5% of steady-state friction value at the assumed initial velocity (see set 1 in Table 1). The slowness law not modified at high velocity was used. The unperturbed time delay (indicated) is 126.2 years unlike Figure 8. This confirms that two different reference states imply different values of the unperturbed time delays, as discussed in section 2.

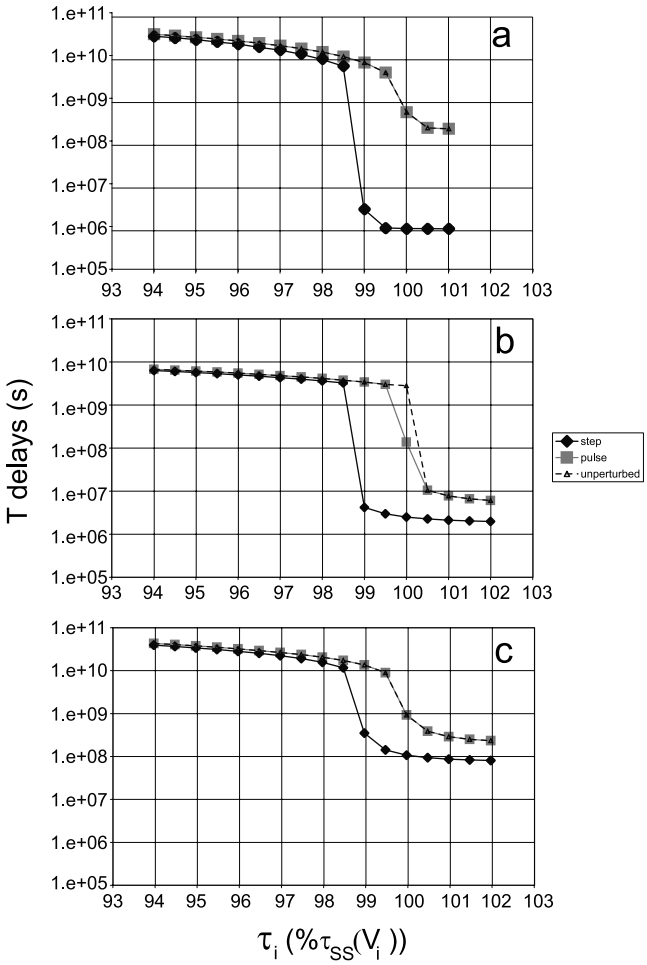

Figure 10. Unperturbed time delay (dashed line with open triangles), triggering delay related to a step of $\Delta\tau_S = 5$ bars (solid black line with solid diamonds) and triggering delay related to a pulse of $\Delta\tau_G = 5$ bars and a duration of $6\sigma = 11.25$ s (solid gray line with solid squares) as a function of the distance of the onset time state from the steady-state line, with the same onset time velocity $V_i \cong V_s$, but different values of the friction value at the onset time $\tau_i \cong \tau_s$ (expressed as a percentage of $\tau_{SS}(V_i) \cong \tau_{SS}(V_s)$). The system condition at the onset time is well approximated by the system conditions at the beginning of the simulation since we perturb the system at few seconds after the beginning of the simulation. The slowness law not modified at high velocity was used. (a, b, and c) Results of simulations using the parameters listed in Table 1 for the sets 1, 2, and 3, respectively. The parameter set 2 in Table 1 can be obtained from the parameters used by *Gomberg et al.* [1998] if a normal stress $\sigma_n = 100$ MPa is assumed.

considered in Figure 10, as well as in Figures 6 and 9, we can exclude the instantaneous triggering effect of the stress pulse (discussed in the previous section and shown in Figure 6) and we have the null effect.

[26] In Figure 10, we note that the unperturbed time delays decrease by orders of magnitude when the OTS is changed from below to above the steady-state line, leaving the other parameters unchanged. This is due to the change in sign of the time derivative of the state variable, which is related to the opposite of the acceleration of the system. Above the steady-state line, the state variable decreases with time and below it increases. If the state variable is a measure of the contact strength area, this implies that during the portion of the cycle above the steady-state line, the fault is weakening and accelerating (see also Figure 3), while below it the fault strengthens. Moreover in Figure 10 we can note that, starting from stress values smaller than the steady-state friction ($\tau_i \leq 98.5\%\ \tau_{SS}(Vi)$), both the triggering delay t_p and the unperturbed time delay t_u are comparable, regardless of the stress perturbation applied. In the case of the permanent stress perturbation, we have that $t_p < t_u$, but both the delays are of the same order of magnitude so that we do not have a strong triggering effect, i.e., the condition $t_p \ll t_u$. This can be explained by considering that in these cases the slider state at the onset time is well below the steady-state curve, and the stress perturbation is not sufficient to overcome or to get very near this boundary. Accordingly the triggering delay is not significantly reduced with respect to the unaltered value related to the same OTS. However, we can note in Figure 10 that, approaching the steady state ($\tau_i > 98.5\%\ \tau_{SS}\ (V_i)$), the triggering delays associated with a stress step tend to become at least two orders of magnitude less than the unperturbed time delay or the triggering delay associated with a stress pulse of the same amplitude. Thus in this case we have a strong triggering effect, $t_p \ll t_u$. This can be explained noting that in this case the stress step, unlike the stress pulse, forces the system to suddenly reach a state above the steady-state line as shown in Figure 8. This is sufficient to reduce the time required to reach an instability starting from this perturbed state, as evident from the results shown in Figure 10 for the unperturbed time delay as a function of the distance from the steady-state line.

[27] The results presented in this section show that the dependence of the triggering delay on the OTS is not limited to the dependence on the velocity at the onset time [see *Dieterich*, 1994]. We point out that in all the simulations shown in Figures 8–10 the velocity value at the onset time is the same, but the frictional stress value is different. We also perturbed the system when it is on the steady-state line, as reported in the following section, assuming different values of the velocity V_i and $\tau_i = \tau_{SS}(V_i)$. In this case and for positive static stress perturbations, t_p is expected to be much smaller than t_u, since the system is always forced to reach a state above the steady-state line after the perturbation. Finally, we perturbed the system when it is on its cycle, namely we identify the OTS in this case as a point of the closed trajectory in the phase plane describing the slider cycle (see Figures 3, 8, and 9).

6. Adopted Constitutive Parameters

[28] In this section we aim to discuss how triggering delays depend on the adopted constitutive parameters for the same external applied loads. We will consider in the following only permanent (step) stress changes, since they are more efficient than transient (pulse) stress changes in changing the state of the system, as shown in previous sections. We are using rate- and state-dependent friction laws, and in this formulation the constitutive parameters are the parameter A, defining the direct effect of friction in the governing equation, and the parameters B and L, which

control the evolution of the state variable. The results of this parametric study are shown in Figure 11. We use the set of parameters listed in Table 1 (set 4) for all the simulations considered here. We assume that at the time of application of the stress perturbation the system is at steady state, which means that the corresponding friction value is defined by the chosen onset time velocity V_i (see equation 4). According to the results of the previous section, this produces a significant triggering effect characterized by triggering delays much shorter than the unperturbed time delays. In this case, the system is accelerating after the stress perturbation. We consider the following theoretical estimate of the triggering delay derived by *Dieterich* [1994] for a slowness evolution law under the hypothesis of close to failure conditions (i.e., an accelerating unstable process)

$$t_p = \frac{A}{\dot{\tau}_0} \ln\left[\frac{\dot{\tau}_0}{(-k + B/L)V_i^+} + 1\right] \tag{7}$$

where $V_i^+ = V(T_0^+) \cong V(T_0) \exp(\Delta\tau_S/A)$, according to equation (5). The results of our simulations are compared in Figure 11 with the theoretical estimates resulting from equation (7).

[29] In Figure 11a, we show the dependence of triggering delays on the stress step amplitude for the reference set of constitutive parameters either considering a Ruina-slip (SL, equation (2)) or a Dieterich-ageing (AL, equation (1)) slowness evolution law, each modified to have a constant value of friction at high slip rates. The resulting unperturbed time delays of the first instability are 2.6×10^7 s (SL) and 3.1×10^7 s (AL), respectively. After about three dynamic instabilities, the system reaches its cycle with a period of 4.3×10^8 s (SL) and 8.8×10^8 s (AL). This confirms that in general the unperturbed time delays are different from the recurrence time of slider instabilities when the system is on its cycle. This difference could not be noticed by previous investigations because they neglect inertia. Figure 11a confirms that the triggering delays are much smaller than the unperturbed time delays. As already demonstrated in Figure 5, the triggering delays obtained with the SL are shorter than those obtained with the AL, and this is due to the stronger restrengthening effect in the evolution equation implicit in the ageing law.

[30] A general result emerging from Figure 11 is that, unlike transient (or pulse) stress perturbations, step stress changes can promote induced instabilities with a variety of triggering delays ($0 \leq t_p \leq t_u$) that depend on the system parameters and the onset time conditions. Moreover, we can note that the values resulting from the slowness law are in good agreement with the predictions from equation (7). This implies that the triggering delay depends only on the velocity value V_i at the onset time. Although this does not represent the general case, as discussed in the previous section, it is a good approximation for the simulations considered here. We recall that in Figure 11 the system is assumed to start from the steady-state friction level, so that after the stress perturbation the state variable decreases monotonically (because the system after the positive stress perturbation is above the steady-state line). This is one of the hypotheses used to derive the theoretical estimate of triggering delay from equation (7).

[31] Assuming an inverse dependence of the triggering delay on the sliding velocity immediately after the induced load application [equation (7) and *Dieterich*, 1994] we expect an exponential decrease of the triggering delay with increasing stress amplitude, which is confirmed by our results (Figure 11a). In the simulations shown in the other panels of Figure 11, we adopted a stress step of 10.4 bars and varied the remaining parameters around the reference values reported in Table 1. Figure 11b shows that the time delay depends inversely on the onset time velocity V_i. We show in this figure the curve $(L/V_i) \exp(-\Delta\tau_S/A)$ as a function of V_i. The resulting time interval would represent the time necessary to slip a distance equal to L with a constant velocity equal to that assumed immediately after the stress application, according to equation (5). This represents an upper estimate of the triggering delay, as evident in Figure 11b, since the slider velocity is increasing with time during the time interval t_p. It is worth noting that, changing the onset time velocity V_i, both t_p and t_u vary (the latter decreases with the onset time velocity remaining of the order 10^7 s), but the period of the slider cycle remains unchanged, since it does not depend on the particular adopted reference state. In Figures 11c and 11d, we represent the dependence of the triggering delay on the parameter A (which accounts for the direct effect of friction) and the critical slip distance L. The dependence of t_p on L is almost linear, in agreement with the results shown by *Roy and Marone* [1996]. The results shown in Figures 11e and 11f suggest that the dependence of t_p on the B parameter and the stiffness k is less important. The unperturbed time delay t_u also remains of the order of 10^7 s when varying A, B, L and k.

[32] It is worth observing that both the unperturbed time delay and the triggering delay are not necessarily defined in the case of the slowness law when the condition $k < (B - A)/L$ (the instability condition) is not verified. In the conditionally stable regime [$k > (B - A)/L$, see *Scholz*, 1990], equation (7) predicts a negative triggering delay if k is larger than B/L. The parametric interval defining those values fulfilling the instability conditions is marked by dashed gray lines in Figure 11 (a gray arrow depicts the domain of parameters satisfying the instability conditions). The use of a slowness law implies that these curves are limited to the unstable regime. This is in agreement with the nonlinear stability analysis made by *Raijnith and Rice* [1999], according to which the previous condition is necessary to have an instability; however, this is not true for the slip law. For the slowness law, we have instabilities in the stable regime only when we reach it by means of an increase of the A parameter (Figure 11c). In the stable regime, the system eventually undergoes only one instability and after that it tends to attain its equilibrium state.

[33] On the basis of the results shown in Figure 11c, we point out that the assumption of a small direct effect of friction (small A) compared to the stress perturbation amplitude is one of the most effective ways to produce a value of $t_p \ll t_u$, i.e., to have relevant triggering effects. Reducing A, in fact, means a larger velocity perturbation for the same amplitude of stress change (equation (5)). We remark that A and B include the effective normal stress, which implies that regions with low effective normal stress or high pore pressures might be more effectively triggered.

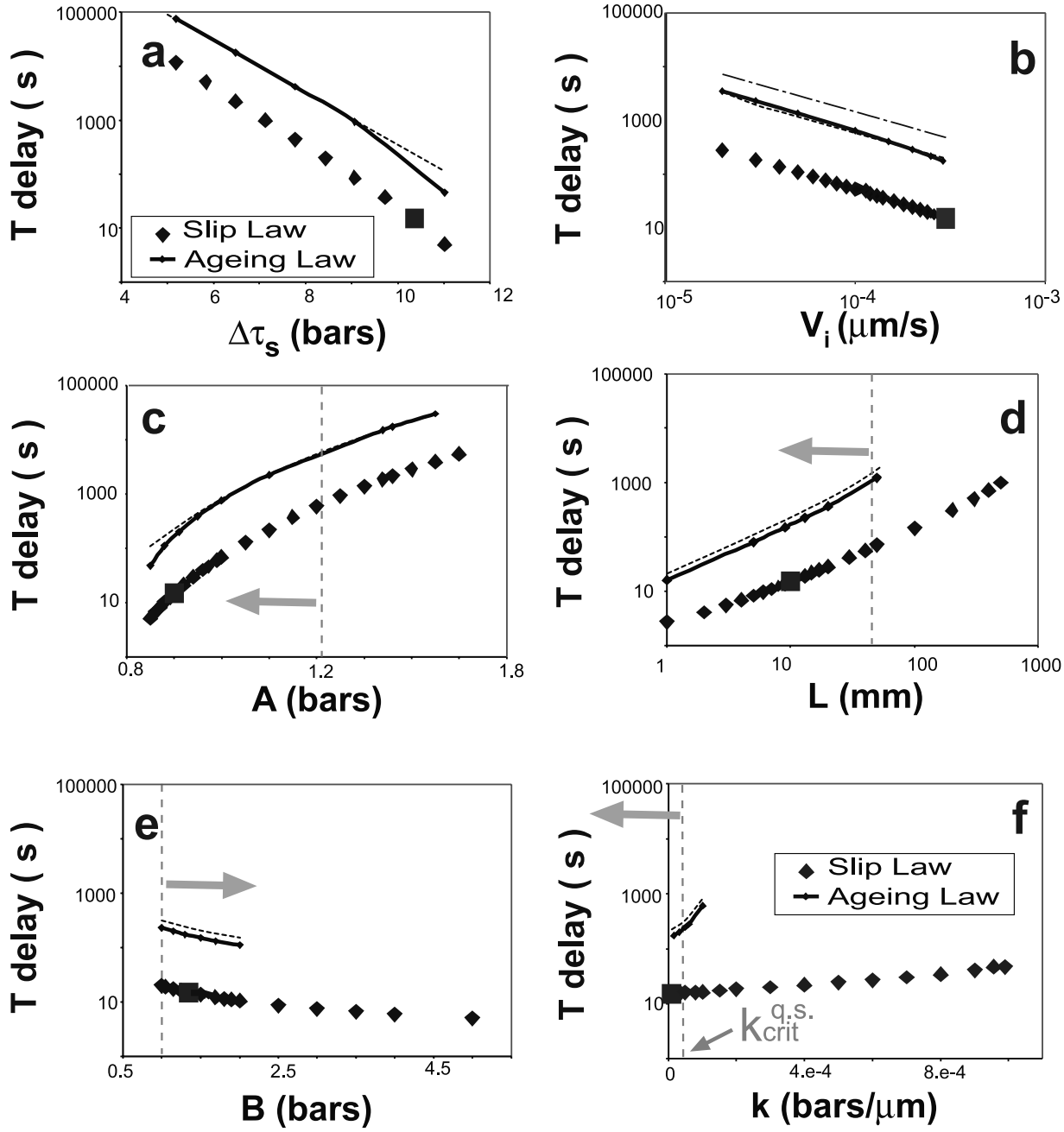

Figure 11. Triggering delays as functions of system parameters, for the slip law and the ageing law not modified at high velocity. The ageing law results are compared with values (dashed line) predicted by equation (7). In each panel, only one parameter is varied assuming all the others fixed. The fixed values of parameters are listed in set 4 of Table 1. The amplitude of the applied static stress perturbation is $\Delta\tau_S =$ 10.4 bars (fixed). The direction of the gray arrows depicts the range of parameters fulfilling the instability conditions ($k < k_{\mathrm{crit}}^{q.s.} \equiv (B - A)/L$), which is also delineated by dashed gray lines. In (b), we also plot (dash-dotted) the approximated dependence of triggering delay on the velocity at the onset time given in the text ($t_p \approx L/V_i$)exp($-\Delta\tau_S/A$). We assume initial conditions on the steady-state line, and we perturb the system a few seconds after the beginning of the simulation so that the velocity at the onset time is $V_i \cong V_s$ and the friction value at the onset time is $\tau_i \cong \tau_{SS}(V_i)$.

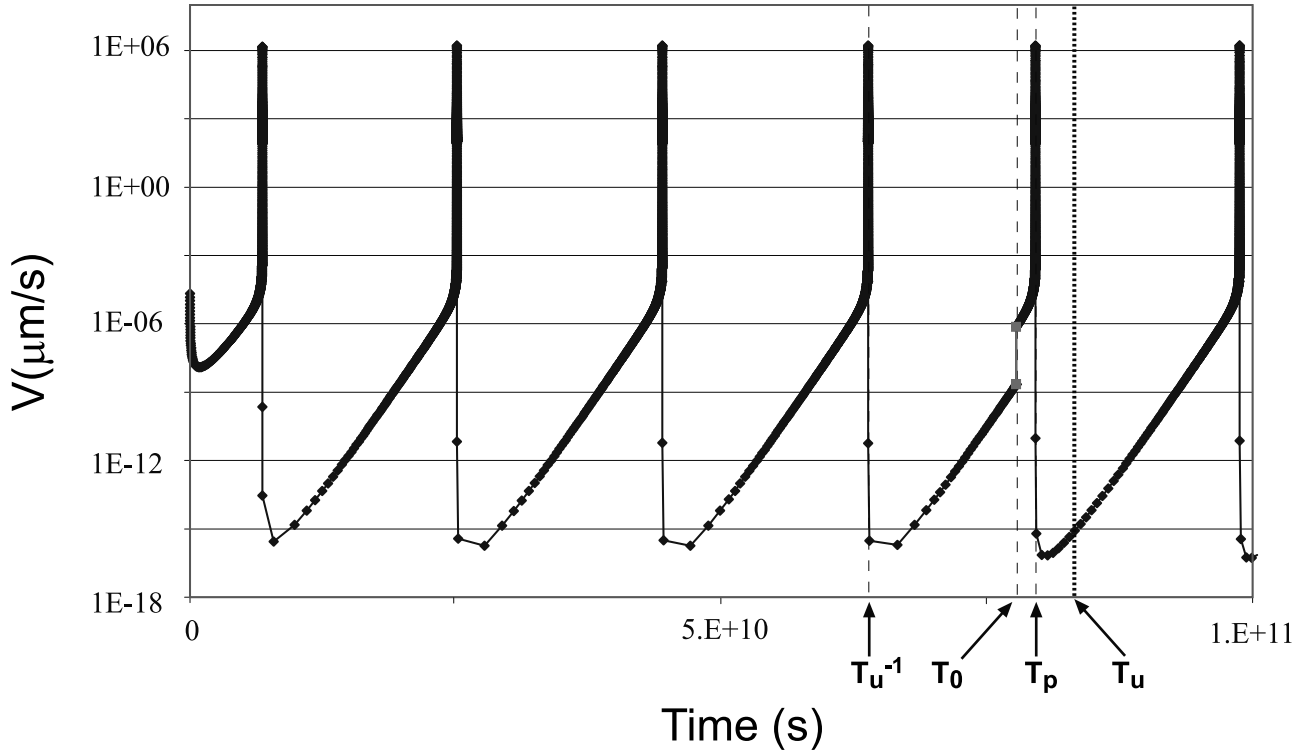

Figure 12. Perturbation of the seismic cycle of the slider represented by its slip velocity time history caused by a static stress change of $\Delta\tau_S = 5.21$ bars. The perturbation is applied on the system trajectory after four instabilities from the beginning of the simulation. The system at the beginning of the simulation is at a friction value equal to 99% of the steady-state friction for the assumed initial velocity. After the first instability, the system tends to lose memory of this initial state. System parameters are listed in set 1 of Table 1 and the slowness law was used. The velocity values at the onset time T_0 and immediately after it are marked by two gray square symbols. The sudden, stepwise increase of velocity caused by the stress perturbation is evident (see also Figures 4 and 8). The first instability after the onset time occurs at a time instant T_p. If the system was not perturbed at T_0, the first subsequent instability would have occurred at an instant of time $T_u > T_p$. The unperturbed occurrence at $t = T_u$ is marked by a dotted line. The cycle period T can be estimated as the distance between two subsequent instabilities occurring in unperturbed conditions, provided that the system lost memory of the initial state (e.g., $T = T_u - T_u^{-1}$). The temporal distance between the last instability preceding the stress perturbation and occurring at the time instant T_u^{-1} and the next one occurring at T_p is markedly less with respect to the cycle period T.

We emphasize that the variability of triggering delays with the parameters A, B and L should be taken into account when interpreting the effect of coseismic stress changes on aftershocks and seismicity rates in the volume surrounding the causative fault.

7. Stress Perturbation Applied on the Seismic Cycle: Dependence on the Onset Time

[34] In the simulations discussed above, we applied the induced perturbation shortly after the beginning of the simulation, and therefore the OTS does not differ from the state assumed at the beginning of the simulation. In this section, we present the results of numerical simulations performed by perturbing the system after the occurrence of several instabilities in order to be sure that the system has lost its memory of the initial state. In this case, the system is perturbed when it is on its cycle and it is possible to associate a particular OTS to a particular stage along the seismic cycle. The system cycle represents a natural set of reference conditions for a fault model: in fact, if the adopted parameters satisfy the instability condition $k < (B - A)/L$ and if the system is subjected only to the tectonic loading rate, the system trajectory tends to attain the cycle. However, the system can also be moved from the cycle if subjected to relevant stress perturbations. Because of the dependence on the system condition at the onset time, shown in previous sections, this can lead to differences in the triggering delays. In this section we aim to discuss the dependence of triggering delays on the onset time T_0, computed from the time of the last instability that occurred in the system cycle before the application of the induced stress perturbation (see Figure 12). We use the slowness law without any constraint at high slip rates with the set of parameters listed in Table 1 and apply a stress step of about 5 bars. Figure 12 shows the sliding velocity as a function of time and emphasizes the effect of the perturbation applied along the cycle. The unperturbed time delay and the triggering delay are compared in Figure 13, where we plot these values as functions of the onset time. We computed

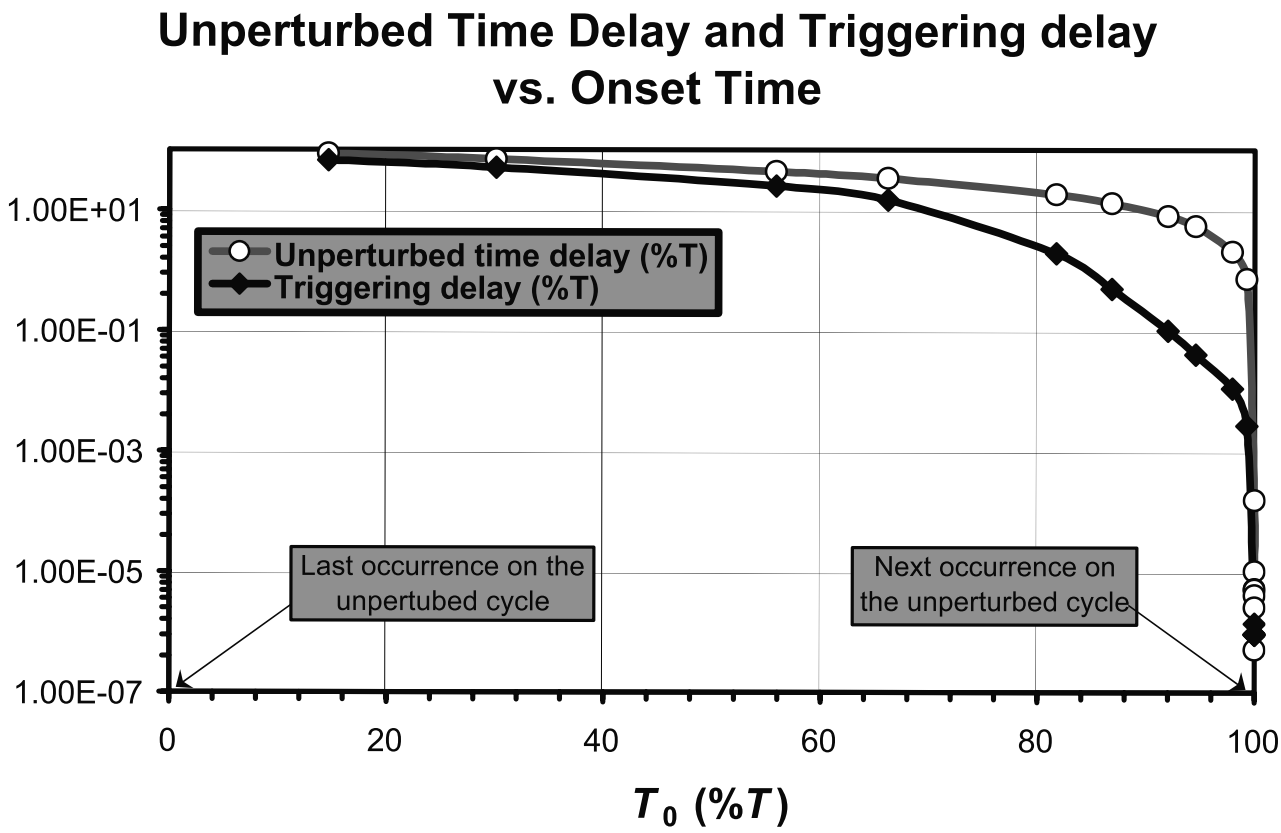

Figure 13. Unperturbed time delay $t_u = T_u - T_0$ (gray line with open circles) and triggering delay $t_p = T_p - T_0$ (black line with solid diamonds) as functions of the onset time T_0 when the static stress perturbation of $\Delta\tau_S = 5.21$ bars is applied along the system cycle, as in Figure 12. We used the slowness law, the parameter values reported in set 1 of Table 1 and the initial friction was 99% of the steady-state friction at the assumed initial velocity. The onset time T_0 is computed with respect to the occurrence time T_u^{-1} of the last instability preceding T_0 in the unperturbed cycle (see Figure 12 for time definitions). The time intervals t_u, t_p, as well as the onset time T_0, are expressed as a percentage of the cycle period $T = T_u - T_u^{-1}$.

the times T_0, T_u, and T_p starting from the time that the last instability (T_u^{-1} in Figure 12) occurred before the application of the stress perturbation. The triggering delay $T_p - T_0$ appears to be smaller than the unperturbed time delay $T_u - T_0$, but in general, they are both comparable for a large fraction of the cycle (T); only if the induced load is applied after 80% of the cycle does the triggering delay become much shorter than the unperturbed time delay. These onset time conditions are equivalent to the ''close to failure conditions'' proposed by *Gomberg et al.* [2000].

[35] The results shown in Figure 13 confirm those obtained by perturbing the system at the beginning of the simulation and discussed in the previous sections. We have plotted in Figure 3 the phase diagram corresponding to the unperturbed cycle where we have indicated with a color scale the temporal evolution of the dynamic system. That figure clearly points out that the slider lies well below the steady-state friction level for most of the cycle (more than 80% of the whole cycle). This explains why induced loads can efficiently trigger dynamic instabilities only when they are applied at the end of the cycle (after 80–90% of temporal evolution). This corresponds to the close to failure conditions, which are characterized by an onset time state of the system (at $t = T_0$) relatively close to or above the steady-state line. The latter condition represents the requirement to have the most efficient triggering phenomena caused by either permanent or transient stress perturbations, i.e., the condition $t_p \ll t_u$. This is consistent with the stability analysis discussed by *Gu et al.* [1984]. Because the system temporal evolution and its cycle depend on the adopted onset time conditions and constitutive parameters, we point out also that the ''close to failure conditions'' depend on system parameters. However, we can exclude a strong triggering effect ($t_p \ll t_u$) if we perturb the system in the first part of the cycle after the last instability.

[36] Our results are in agreement with those obtained by *Gomberg et al.* [1998, 2000]. However, unlike previous studies, we can apply the external load on the true cycle of the system and not on a transient trajectory leading to the first instability (the only instability that can be obtained with a quasi-static approximation). Since in previous studies the close to failure conditions have been evaluated on this trajectory and the unperturbed occurrence time T_u was identified with the cycle time, our results allow us to identify more properly the conditions for a strong triggering effect ($t_p \ll t_u$) when the fault is considered on its cycle. As an example, our results further restrict the range of close to failure conditions found by *Gomberg et al.* [1998]. She

obtained a significant triggering effect ($t_p/t_u < 0.4$) when perturbing the system at $T_0 \geq 87\%\ T_u$, where T_0 and T_u were counted from the beginning of the simulation (see Figure 5 of that paper). Using the corresponding system parameters, as in set 2 of Table 1, and a static stress change of similar amplitude, we obtain an equivalent effect only when $T_0 \geq 99\%\ T$, where T_0 was counted from the last instability instant (T_u^{-1}) and T is the cycle period.

8. Discussion and Concluding Remarks

[37] In order to model earthquake triggering by static and transient stress changes, we investigate in the present study the dynamic response of a simple analog system (a spring-slider obeying rate and state-dependent friction) to a sudden stress perturbation represented either as a step or a pulse. We estimate the time interval separating the application of the induced stress perturbation from the subsequent dynamic instability (the triggering delay t_p) and the time of failure under unperturbed conditions (t_u). For a given applied load, we analyze the dependence of triggering delays on different constitutive parameters and mechanical conditions at the time of the application of the stress perturbation. According to our results, we can conclude that, in the framework of validity of such a simple spring-slider system, the mechanisms underlying earthquake triggering by dynamic and static stress perturbations are different. In general, dynamic stress changes cause induced instabilities only with very short triggering delays or do not produce relevant modifications to the temporal system evolution. Static stress changes, in principle, can promote induced instabilities with a wide variety of triggering delays.

[38] We have shown that this difference is intrinsic to the dynamic response of the slider to permanent (static) and transient (dynamic) applied stress changes. An important conclusion emerging from our simulations is that the value of the triggering delay strongly depends on the state of the spring-slider dynamic system reached immediately after the stress perturbation. Only if this state is significantly different from that characterizing the system at the time of application of the external perturbation (or onset time) do we have differences between the triggering delay and the unperturbed time delay. This explains the different response of the system to dynamic and static stress perturbations of the same amplitude for the same system parameters and system conditions at the onset time. Unlike static stress changes, dynamic stress changes are generally unable to significantly perturb the state of the system and generally tend to produce a ''null'' triggering effect ($t_p \approx t_u$). This conclusion is quite original with respect to previous investigations.

[39] It has been already pointed out by previous investigations that, while negative static stress changes can delay the occurrence of induced instabilities, negative dynamic stress changes do not produce any perturbing effect. Our results can provide an explanation of this problem, because only permanent stress perturbations are able to significantly change the mechanical conditions of the dynamic system (the slider in our simulations) and therefore modify (advance or delay) the time of occurrence of the impending failure. While a negative static step is able to move the system far away from the steady state and to maintain this position through time, a dynamic transient stress perturbation (positive or negative) is generally unable to permanently modify the state of the system, unless is positive and large enough to induce a nearly instantaneous failure occurring at times comparable with the duration of the external perturbation.

[40] From the results shown in the previous sections, the triggering delay and the unperturbed time delay are strongly affected by the state of the spring-slider dynamic system at the time of application of the external perturbation. In the framework of the rate and state formulations, this state is not completely specified only by the sliding velocity value but it depends also on the value of the state variable in quasi-static conditions. This implies that the triggering delay does not depend only on the velocity at the onset time, unless the system is already accelerating to a failure (the so-called close-to-failure conditions), as considered by *Dieterich* [1994]. In our study we demonstrate that, in order to have a significant triggering effect $t_p \ll t_u$, it is necessary that the onset time state of the system is relatively close to or above the steady-state level.

[41] We have analyzed the slider response to stress perturbations applied either at the beginning of the simulations or after several instabilities, when the slider is on its cycle. The application of the induced perturbation along the cycle represents an attempt to consider natural onset time conditions for a tectonic fault. Our analysis confirms that only for particular onset time conditions the triggering effect is relevant ($t_p \ll t_u$). Our results suggest that the likelihood to promote an induced failure is large only if the fault is toward the end of its cycle. The application of the induced load during the cycle, instead of at the beginning of the simulation, allowed us to properly define the range of close to failure conditions. This range of relevant triggering effect ($t_p \ll t_u$) is restricted with respect to the results of previous investigations [see *Gomberg et al.*, 1998, 2000]. The range of close-to-failure configurations leading to strong triggering effects depends on system parameters, but it turns out to be smaller than the ultimate 10% of the cycle before the unperturbed instability, for the system parameters and stress perturbations amplitudes considered here. These results can provide an appropriate explanation of the similarity between Coulomb-like triggering behavior implicit in the rate and state formulation [see *Gomberg et al.*, 2000]. The result that dynamic stress changes only cause short triggering delays is consistent with those of *Voisin* [2001], who studied earthquake triggering by applying transient stress perturbations to a 2-D antiplane finite fault obeying a slip-dependent constitutive law.

[42] The triggering delays (or clock advances) also depend on the adopted constitutive parameters, on the assumed constitutive law and on the stress amplitude. Unfortunately, the lack of knowledge of the mechanical state of a fault, the expected heterogeneity of constitutive parameters and the difficulties in constraining the time history of the induced stress field make the prediction of the dynamic response of actual faults a very difficult task. *Harris and Simpson* [1998] have shown that a wide range of constitutive parameters in the rate and state friction formulation could satisfy the seismicity rate change in $M \sim 6$ earthquakes from before to after the great (M 7.8) 1906 San Francisco earthquake. This implies that triggering delays estimated for single earthquake pairs do not constrain fault constitutive properties, and that we have to focus on the

effects of stress perturbations on fault populations [as suggested by *Dieterich*, 1994]. Moreover the effects of heterogeneity of constitutive parameters should be taken into account when interpreting the effects of coseismic stress changes on seismicity rate changes, on the rate of aftershock production and on aftershock patterns.

[43] *Gomberg* [2001] presented a stimulating discussion on the limitations and failures of earthquake failure models to explain triggering of seismicity by dynamic stress changes. She suggests that "accelerating" earthquake failure models (including rate and state friction laws) do not predict the finite durations of sequences triggered by dynamic stress changes. According to our results, both static and dynamic stress changes can induce failures on those secondary faults that are already at end of their cycle as well as those that are already nucleating at the time of application of the induced load. For short time windows after an earthquake, both dynamic and static stress changes act together to promote failures. In the near field, the effect of static and dynamic stress changes is indistinguishable, then both static and dynamic stress changes are expected to modify the rate of aftershock production. However, according to the results presented in the previous sections, it emerges that the term "triggering" can be properly used in a broad meaning only for those perturbations that are able to permanently modify the mechanical conditions (the stress state) of dynamic systems (active faults). In these cases, we expect the triggering delay t_p is of finite size and significantly different from the time of failure under unperturbed conditions t_u, depending on the different system conditions at the onset time and constitutive parameters. Therefore permanent stress changes seem to be necessary to explain the observed temporal decay of aftershocks (or the Omori law). This is in agreement with the good explanation provided by static triggering models of many observations, such as the Omori law [e.g., *Dieterich*, 1994]. If some observational evidence of dynamic triggering is in contrast with the results of this study, for instance, if a finite triggering delay is actually observed at remote distances from the inducing seismic event, we are inclined to believe that this is a consequence of the incompleteness of the model used for dynamic triggering (a spring slider simply perturbed by a stress pulse), rather than a failure of the adopted constitutive law.

Appendix A

[44] Using the quasi-static approximation of the spring-slider equation of motion and the governing equation for friction, we can derive the following equation

$$\tau + \Delta\tau(t) = \tau_* + A \ln\left(V/V_*\right) + \Theta \qquad \text{(A1)}$$

where Θ is the state variable for the slip evolution equation that corresponds to $\Theta = B \ln (\xi V_*/L)$ for a slowness evolution law. The factor $A = a\sigma_n$ accounts for the direct effect of friction, and σ_n is the normal stress. Then, from equation (A1) we get

$$V = V_* \exp\left(\frac{\tau + \Delta\tau(t) - \tau_* - \Theta}{A}\right) \qquad \text{(A2)}$$

Assuming $\Delta\tau(t) = 0$ for $t \le T_0$ and $V = V_i$, $\tau = \tau_i$ and $\Theta = \Theta_i$ for $t = T_0$, we can rewrite equation (A2) as

$$V_i = V_* \exp\left(\frac{\tau_i - \tau_* - \Theta_i}{A}\right), \quad \text{for } t = T_0 \qquad \text{(A3)}$$

By dividing equation (A2) by (A3) we have

$$V = V_i \exp\left(\frac{\tau - \tau_i - \Theta + \Theta_i + \Delta\tau(t)}{A}\right) \quad \text{for } t \ge T_0 \qquad \text{(A4)}$$

We now indicate as $t = T_0^+$ the end of stress perturbation, corresponding to $\Delta\dot{\tau}(t) = 0$ for $t \ge T_0^+$. If we assume that for $T_0 \le t \le T_0^+$ the elastic traction variation $\tau - \tau_i$ and the state variable variation $\Theta - \Theta_i$ are negligible, then we have from equation (A4) that

$$V \cong V_i \exp\left(\frac{\Delta\tau(t)}{A}\right) \quad \text{for } T_0 \le t \le T_0^+ \qquad \text{(A5)}$$

The two assumptions leading to equation (A5) are valid if the system at $t = T_0$ is close to the steady-state value, if the system velocity and the loading point velocity (V_i and V_0) are relatively low (for instance, when they are comparable to the plate velocity value, $\le$0.1 m/yr) and if the duration of the perturbation $T_0^+ - T_0$ is of the order of several seconds, as is the time interval characterizing the stress perturbation variation in our study. Therefore equation (A5) shows that the velocity follows closely the applied stress perturbation in the time interval during which $\Delta\tau(t)$ varies.

[45] If we now assume $\Delta\dot{\tau}(t) = 0$, which corresponds to unaltered conditions or to perturbed conditions for $t \ge T_0^+$, and we take the time derivative of equation (A1), we obtain

$$\dot{V} = \frac{V}{A}\left(\dot{\tau} - \dot{\Theta}\right) \quad \text{for } t \ge T_0^+ \qquad \text{(A6)}$$

Considering $\dot{\Theta} \neq 0$ (we are not exactly at the steady state), we can write

$$\dot{V} = -\frac{V\dot{\Theta}}{A}\left(1 - \frac{\dot{\tau}}{\dot{\Theta}}\right), \quad \text{for } t \ge T_0^+ \qquad \text{(A7)}$$

Because V and A are positive, if $\dot{\tau}/\dot{\Theta} < 1$, then equation (A7) shows that the slip acceleration $\dot{V}$ has the opposite sign of $\dot{\Theta}$. This means that after the end of the stress perturbation the system accelerates (or decelerates) if the state of the system is above (or below) the steady-state line in the phase plane (V, τ_f).

[46] **Acknowledgments.** We wish to thank Joan Gomberg, Maurizio Bonafede, and Ross Stein for helpful discussions and Enzo Boschi who stimulated our collaboration. We are indebted to Joan Gomberg, Ruth Harris, Sandy Steacy, and Teruo Yamashita who reviewed the manuscript; their comments and criticisms were important to substantially improve the paper. This study has been partially supported by the European Community contract EVG1-CT-1999-00001, project PRESAP.

References

Beeler, N. M., T. E. Tullis, and J. D. Weeks, The roles of time and displacement in the evolution effect in rock friction, *Geophys. Res. Lett.*, *21*, 1987–1990, 1994.

Belardinelli, M. E., M. Cocco, O. Coutant, and F. Cotton, Redistribution of dynamic stress during coseismic ruptures: Evidence for fault interaction and earthquake triggering, *J. Geophys. Res.*, *104*, 14,925–14,945, 1999.

Boatwright, J., and M. Cocco, Frictional constraints on crustal faulting, *J. Geophys. Res.*, *101*, 13,895–13,910, 1996.

Brodsky, E. E., V. Karakostas, and H. Kanamori, A new observation of dynamically triggered regional seismicity: Earthquakes in Greece following the August, 1999 Izmit, Turkey earthquake, *Geophys. Res. Lett.*, *27*, 2741–2744, 1999.

Cotton, F., and O. Coutant, Dynamic stress variations due to shear faults in a plane-layered medium, *Geophys. J. Int.*, *128*, 676–688, 1997.

Dieterich, J. H., Modeling of rock friction, 1, Experimental results and constitutive equations, *J. Geophys. Res.*, *84*, 2161–2168, 1979.

Dieterich, J. H., A model for the nucleation of earthquake slip, in *Earthquake Source Mechanics*, *Geophys. Monogr. Ser.*, vol. 37, edited by S. Das, J. Boatwright, and C. H. Scholz, pp. 37–47, AGU, Washington, D. C., 1986.

Dieterich, J. H., A constitutive law for rate of earthquake production and its application to clustering, *J. Geophys. Res.*, *99*, 2601–2618, 1994.

Gomberg, J., The failure of earthquake failure models, *J. Geophys. Res.*, *106*, 16,253–16,263, 2001.

Gomberg, J., M. L. Blanpied, and N. M. Beeler, Transient triggering of near and distant earthquakes, *Bull. Seismol. Soc. Am.*, *87*, 294–309, 1997.

Gomberg, J., N. M. Beeler, M. L. Blanpied, and P. Bodin, Earthquake triggering by transient and static deformations, *J. Geophys. Res.*, *103*, 24,411–24,426, 1998.

Gomberg, J., N. Beeler, and M. Blanpied, On rate-state and Coulomb failure models, *J. Geophys. Res.*, *105*, 7557–7871, 2000.

Gu, J. C., J. Rice, A. L. Ruina, and S. T. Tse, Slip motion and stability of a single degree of freedom elastic system with rate and state dependent friction, *J. Mech. Phys. Solids*, *32*, 167–196, 1984.

Harris, R., Introduction to special section: Stress triggers, stress shadows, and implications for seismic hazard, *J. Geophys. Res.*, *103*, 24,347–24,358, 1998.

Harris, R., and R. W. Simpson, Suppression of large earthquakes by stress shadows: A comparison of Coulomb and rate and state failure, *J. Geophys. Res.*, *103*, 24,439–24,451, 1998.

Hill, D. P., et al., Seismicity remotely triggered by the magnitude 7.3 Landers, California, earthquake, *Science*, *260*, 1617–1623, 1993.

Kilb, D., J. Gomberg, and P. Bodin, Earthquake triggering by dynamic stresses, *Nature*, *408*, 570–574, 2000.

King, G. C. P., and M. Cocco, Fault interaction by elastic stress changes: New clues from earthquake sequences, *Adv. Geophys.*, *44*, 1–38, 2000.

Raijnith, K., and J. R. Rice, Stability of quasi-static slip in single degree of freedom elastic system with rate and state dependent friction, *J. Mech. Phys. Solids*, *47*, 1207–1218, 1999.

Rice, J. R., and J. Gu, Earthquake after effects and triggered seismicity phenomena, *Pure Appl. Geophys.*, *121*, 187–219, 1983.

Rice, J. R., and S. T. Tse, Dynamic motion of a single degree of freedom system following a rate and state dependent friction law, *J. Geophys. Res.*, *91*, 521–530, 1986.

Roy, M., and C. Marone, Earthquake nucleation on model faults with rate- and state-dependent friction: Effects of inertia, *J. Geophys. Res.*, *101*, 13,919–13,932, 1996.

Ruina, A. L., Friction laws and instabilities: A quasi-static analysis of some dry frictional behaviour, Ph.D. thesis, Brown Univ., Providence, R. I., 1980.

Ruina, A. L., Slip instabilities and state variable friction laws, *J. Geophys. Res.*, *88*, 10,359–10,370, 1983.

Rybicki, K., T. Sato, and K. Kasahara, Mechanical interaction between neighboring active faults: Static and dynamic stress field induced by faulting, *Bull. Earthquake Res. Inst. Univ. Tokyo*, *60*, 1–21, 1985.

Scholz, C. H., *The Mechanics of Earthquakes and Faulting*, Cambridge Univ. Press, New York, 1990.

Scholz, C. H., Earthquakes and friction laws, *Nature*, *391*, 37–42, 1998.

Stein, R. S., The role of stress transfer in earthquake occurrence, *Nature*, *402*, 605–609, 1999.

Voisin, C., Dynamic triggering of earthquakes: The linear slip-dependent friction case, *Geophys. Res. Lett.*, *28*, 3357–3360, 2001.

Weeks, J. D., Constitutive laws for high-velocity frictional sliding and their influence on stress drop during unstable slip, *J. Geophys. Res.*, *98*, 17,637–17,648, 1993.

M. E. Belardinelli and A. Bizzarri, Dipartimento di Fisica, University of Bologna, Settore di Geofisica, Viale Berti-Pichat 8, 40127 Bologna, Italy. (elina@ibogfs.df.unibo.it)

M. Cocco, Istituto Nazionale di Geofisica e Vulcanologia, Via di Vigna Murata 605, 00143 Rome, Italy.